Cell

Transcriptional Control of Gene Expression by MicroRNAs

Basel Khraiwesh,[1,4,5,6] M. Asif Arif,[1,5] Gotelinde I. Seumel,[1,3] Stephan Ossowski,[2] Detlef Weigel,[2] Ralf Reski,[1,3,4,*] and Wolfgang Frank[1,3,*]

[1]Plant Biotechnology, Faculty of Biology, University of Freiburg, Schaenzlestrasse 1, 79104 Freiburg, Germany
[2]Department of Molecular Biology, Max Planck Institute for Developmental Biology, 72076 Tuebingen, Germany
[3]Freiburg Initiative for Systems Biology (FRISYS), Schaenzlestrasse 1, 79104 Freiburg, Germany
[4]Centre for Biological Signalling Studies, Albertstrasse 19, 79104 Freiburg, Germany
[5]These authors contributed equally to this work
[6]Present address: Department of Plant Systems Biology, Flanders Institute for Biotechnology and Department of Plant Biotechnology and Genetics, Ghent University, Technologiepark 927, 9052 Gent, Belgium
*Correspondence: ralf.reski@biologie.uni-freiburg.de (R.R.), wolfgang.frank@biologie.uni-freiburg.de (W.F.)
DOI 10.1016/j.cell.2009.12.023

SUMMARY

MicroRNAs (miRNAs) control gene expression in animals and plants. Like another class of small RNAs, siRNAs, they affect gene expression post-transcriptionally. While siRNAs in addition act in transcriptional gene silencing, a role of miRNAs in transcriptional regulation has been less clear. We show here that in moss *Physcomitrella patens* mutants without a *DICER-LIKE1b* gene, maturation of miRNAs is normal but cleavage of target RNAs is abolished and levels of these transcripts are drastically reduced. These mutants accumulate miRNA:target-RNA duplexes and show hypermethylation of the genes encoding target RNAs, leading to gene silencing. This pathway occurs also in the wild-type upon hormone treatment. We propose that initiation of epigenetic silencing by DNA methylation depends on the ratio of the miRNA and its target RNA.

INTRODUCTION

Small RNAs (sRNAs) are potent regulators of posttranscriptional and transcriptional gene expression (Carthew and Sontheimer, 2009; Voinnet, 2009). In plants, miRNAs produced from hairpin-like precursor transcripts are also required for the biogenesis of *trans*-acting small interfering RNAs (ta-siRNAs). Both miRNAs and ta-siRNAs regulate mRNA stability and translation. Another class of sRNAs, siRNAs, processed from perfectly double-stranded RNA (dsRNA), posttranscriptionally silence transposons, viruses, and transgenes and are important for DNA methylation (Baulcombe, 2004; Matzke et al., 2007). Evidence for a similar function of microRNAs (miRNAs) in DNA methylation is limited. The biogenesis of sRNAs from dsRNA is catalyzed by Dicer proteins. The number of different Dicer proteins varies between organisms, reflecting different degrees of specialization. For example, in *D. melanogaster*, Dcr1 produces miRNAs from hairpin precursors, whereas Dcr2 generates siRNAs from dsRNA (Tomari and Zamore, 2005), while in *C. elegans* the only Dicer protein produces sRNAs from different dsRNA triggers (Duchaine et al., 2006). Besides their function in dicing dsRNA, animal Dicers together with accessory proteins act in RNA-induced silencing complex (RISC) or RISC loading complexes (Doi et al., 2003; Pham et al., 2004). Thus, Dicer proteins are also essential components in the executive phase of RNA interference (RNAi), indicating that miRNA/siRNA processing and target RNA cleavage are coupled.

In the seed plant *A. thaliana*, four Dicer proteins (AtDCL1–4) act in different sRNA pathways (Gasciolli et al., 2005; Henderson et al., 2006). The maturation of miRNAs from imperfect RNA foldbacks relies on AtDCL1. In consequence, *Atdcl1* mutants show reduced miRNA levels and increased target mRNA levels, resulting in multiple developmental defects (Golden et al., 2002; Park et al., 2002). AtDCL2 mediates the generation of siRNAs from exogenous RNA (Xie et al., 2004), AtDCL3 acts in the formation of heterochromatin-associated endogenous siRNAs (Herr et al., 2005; Xie et al., 2004), and AtDCL4 is needed for the formation of ta-siRNAs acting in cell-to-cell transmission of silencing signals (Dunoyer et al., 2005; Xie et al., 2005).

A moss, *Physcomitrella patens*, likewise harbors four DCL proteins (Axtell et al., 2007). PpDCL1a and PpDCL1b are similar to AtDCL1. PpDCL3 and PpDCL4 are orthologs of AtDCL3 and AtDCL4, whereas an AtDCL2 ortholog is lacking. Like *AtDCL1*, the primary *PpDCL1a* transcript harbors an intronic miRNA precursor, suggesting a conserved autoregulatory control (Axtell et al., 2007). We created null mutants of *PpDCL1a* and *PpDCL1b*, respectively, by reverse genetics. Their analysis revealed significant functional differences between both proteins and suggest a feedback control of gene expression involving miRNAs and DNA methylation.

RESULTS

Requirement of *PpDCL1a* for miRNA Biogenesis

Utilizing efficient gene targeting in *P. patens* (Strepp et al., 1998), we generated two *PpDCL1a* null mutants (Δ*PpDCL1a*) (Figure S1

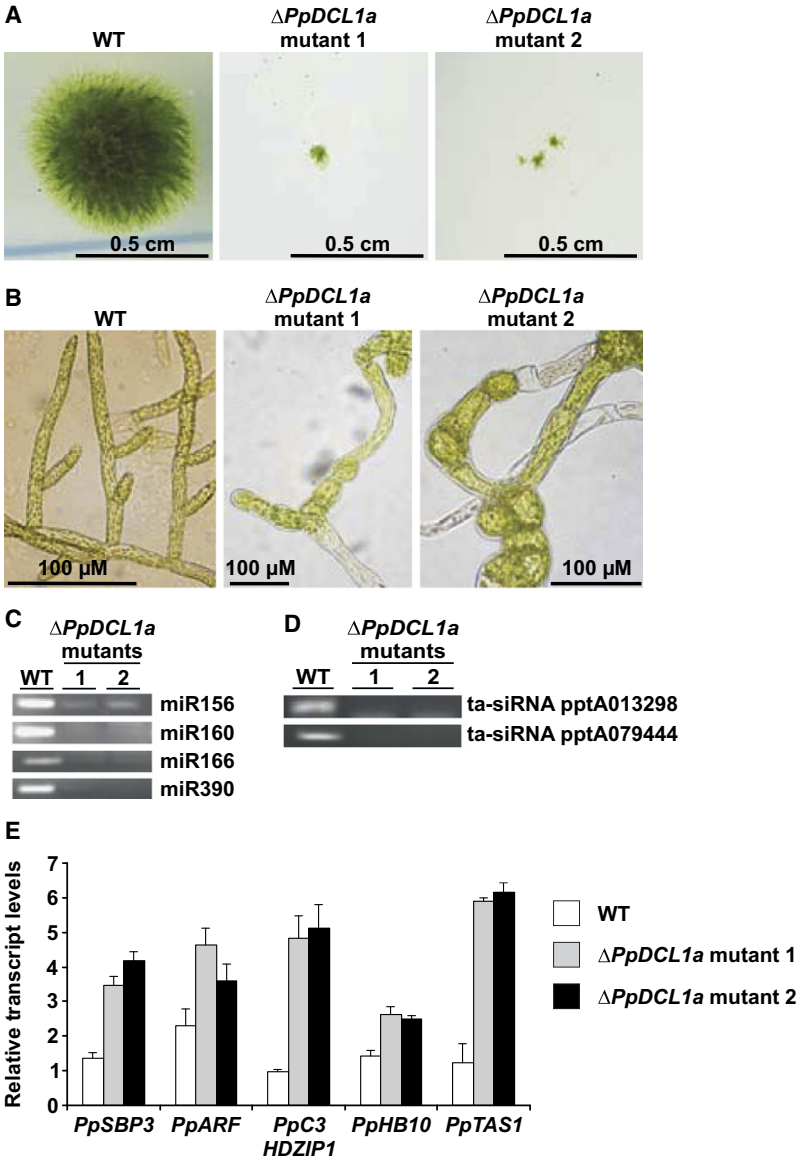

Figure 1. Analysis of Δ*PpDCL1a* Mutants

(A) Protonema of identical density from the WT and two Δ*PpDCL1a* mutants grown for 28 days on solid medium.

(B) Protonema grown in liquid culture.

(C) RT-PCR of miR156, 160, 166, and 390.

(D) RT-PCR of ta-siRNAs pptA013298 (from *PpTAS3*) and pptA079444 (from *PpTAS1*).

(E) Semiquantitative RT-PCR of miRNA targets in the WT and Δ*PpDCL1a*. Bars indicate standard errors (n = 3). See Figure S1 for further molecular analyses and Figure S2 for phenotypic comparison with Δ*PpDCL1b* mutants.

available online). Loss of PpDCL1a resulted in developmental disorders and abnormalities in cell size and shape. Growth of the mutants was severely retarded on minimal medium but slightly better when supplied with vitamins and glucose. In all conditions, Δ*PpDCL1a* were developmentally arrested at the filamentous protonema and did not form leafy stems (Figures 1A and 1B, and Figures S2G and S2H).

To test miRNA biogenesis in these barely growing mutants, we analyzed the accumulation of miR156, 160, 166, and 390 (Arazi et al., 2005; Fattash et al., 2007) by RT-PCR (Varkonyi-Gasic et al., 2007) and sequenced the products as a control. Levels of miR156, 160, and 166 were drastically reduced and miR390 was undetectable in Δ*PpDCL1a* (Figure 1C). In *P. patens*, ta-siRNA precursors (*PpTAS1–4* RNAs) are cleaved at two distinct miR390 target sites. Subsequently, dsRNAs are generated and processed in a phased manner to generate ta-siRNAs (Axtell et al., 2006; Talmor-Neiman et al., 2006). Two ta-siRNAs (pptA079444 from *PpTAS1* and pptA013298 from *PpTAS3*) (Axtell et al., 2006) were present in the wild-type (WT) but absent in Δ*PpDCL1a* (Figure 1D), indicating that lack of miR390 abolishes ta-siRNA production. To test whether reduced miRNAs levels result in elevated levels of target mRNAs, as described for *A. thaliana dcl1* mutants, we analyzed miR156 target *PpSBP3* (Arazi et al., 2005), miR166 targets *PpC3HDZIP1* and *PpHB10* (Axtell et al., 2007; Floyd and Bowman, 2004), miR160 target *PpARF* (Fattash et al., 2007), and miR390 target *PpTAS1* (Axtell et al., 2006). All target RNAs accumulated to higher levels in Δ*PpDCL1a* (Figure 1E), revealing that PpDCL1a is the major *P. patens* DCL protein for miRNA biogenesis and thus the functional equivalent of AtDCL1.

Requirement of *PpDCL1b* for miRNA-Guided Target Cleavage

To test possible redundancies between the two DCL1 homologs in moss, we additionally generated four *PpDCL1b* null mutants (Δ*PpDCL1b*) (Figure S2). These were affected in cell division, growth polarity, cell size, cell shape, and differentiation (Figure 2A and Figure S3A). In contrast to Δ*PpDCL1a*, Δ*PpDCL1b* grew faster and developed some malformed leafy stems (Figure 2B and Figure S3B). Thus, albeit Δ*PpDCL1a* and Δ*PpDCL1b* exhibited severe defects, their phenotypes differed (Figures S2G and S2H).

The levels of six different miRNAs (miR156, 160, 166, 390, 535, and 538) (Arazi et al., 2005; Fattash et al., 2007) in Δ*PpDCL1b* were like in the WT (Figures 2C–2E), revealing that PpDCL1b is not pivotal for miRNA maturation and that the strong mutant phenotype does not result from abolished miRNAs. Subsequently, cleavage of the miRNA targets *PpARF*, *PpC3HDZIP1*, *PpHB10*, and *PpSBP3* in the WT was verified by 5′ RACE, complementary DNA (cDNA) cloning, and sequencing (Figure 3A). An mRNA (*PpGNT1*) (Koprivova et al., 2003) that is no miRNA target served as control (Figure 3A). Although Δ*PpDCL1b* accumulated normal levels of miRNAs, miRNA targets were not cleaved (Figure 3A), revealing a surprising requirement of PpDCL1b for miRNA-guided RNA cleavage.

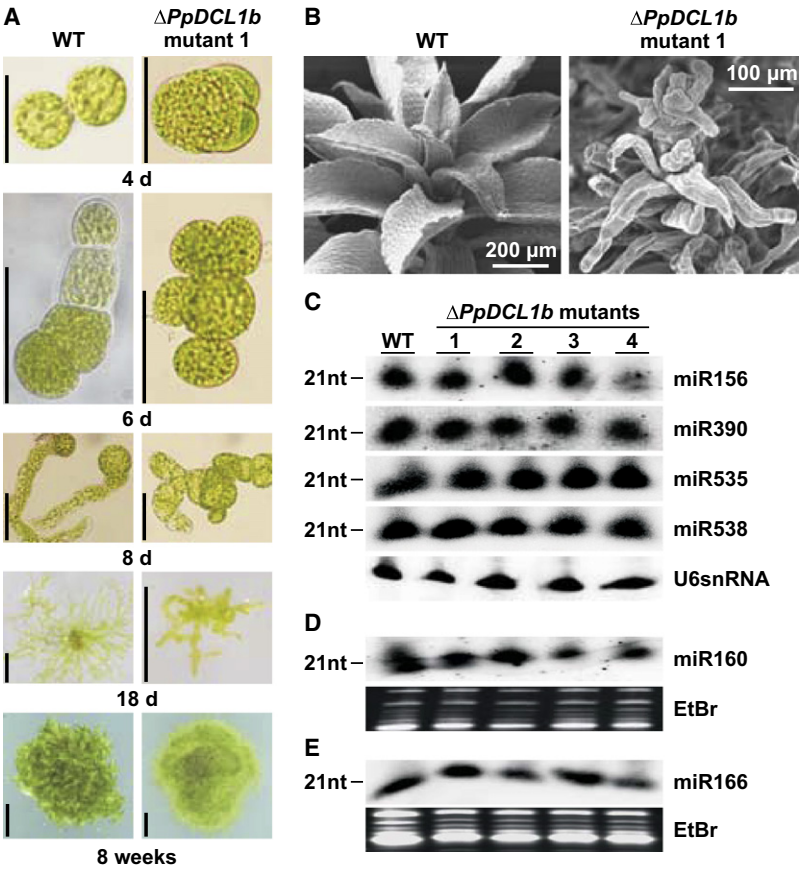

Figure 2. Analysis of Δ*PpDCL1b* Mutants

(A) Regeneration of protoplasts from the WT and Δ*PpDCL1b* mutant 1 over indicated time points. Scale bars represent 100 μm, or 500 μm for the 18-day-old and 8-week-old plants

(B) Scanning electron micrographs of gametophores.

(C) RNA blots with 30 μg total RNA from protonema probed for miR156, miR390, miR535, and miR538. An antisense probe for U6snRNA served as loading control.

(D) RNA blot with 80 μg total RNA from protonema treated with 5 μM auxin (NAA) for 8 hr probed for miR160.

(E) RNA blot with 80 μg total RNA from gametophores probed for miR166. EtBr staining served as a loading control at the bottom of (D) and (E).

See Figure S2 for further molecular analyses, complete images of blots including size markers, and phenotypic comparison with Δ*PpDCL1a* mutants and Figure S3 for phenotypes of other Δ*PpDCL1b* mutants.

Generation of Transitive siRNA Triggered by miRNA-Guided Transcript Cleavage

In the WT, we detected 5′ RACE products resulting from miRNA-guided cleavage of target RNA, as well as various shorter and longer products (Figure 3A). Analogous to other plants, where targeting of transcripts with dsRNA-derived siRNAs or multiple miRNAs (Axtell et al., 2006; Howell et al., 2007; Vaistij et al., 2002) causes production of secondary siRNAs, the miRNA cleavage products detected here may serve as templates for synthesizing cRNA by RNA-dependent RNA polymerase (RdRP). Subsequently, dsRNAs may be processed into secondary siRNAs that spread the initial trigger (Figure 3B). In seed plants, this phenomenon, known as transitivity, was rarely observed in miRNA-based regulation of gene expression (Axtell et al., 2006; Howell et al., 2007) but may be more prevalent than suspected (Luo et al., 2009). In accordance with possible transitivity in *P. patens*, we could synthesize cDNAs from sense and antisense strands of miRNA target mRNAs (*PpARF* and *PpC3HDZIP1*), indicating the presence of dsRNA, in the WT but not in Δ*PpDCL1b* (Figure 3C). To determine whether transitive siRNAs were generated from these dsRNAs, we performed RNA blots with probes for sequences upstream and downstream of the miRNA targeting site. Small RNAs corresponding to sense and antisense strands of *PpARF* and *PpC3HDZIP1* mRNAs were present in the WT but not in Δ*PpDCL1b* (Figure 3D and Figure S4).

Thus, in *P. patens*, transitive siRNAs arise from regions upstream as well as downstream of the miRNA targeting motif after cleavage of mRNAs. These siRNAs most likely target mRNAs at additional sites, thus generating the additional fragments observed by 5′ RACE. We did neither detect siRNAs in Δ*PpDCL1b* or for a control mRNA (*PpGNT1*) in the WT (Figures 3C and 3D), revealing that generation of transitive siRNAs depends on PpDCL1b and is specific for RNAs subject to miRNA-directed cleavage. Biogenesis of these transitive siRNAs involves RdRP-dependent formation of dsRNA precursors as we could synthesize cDNA from the antisense strand of miRNA target transcripts (Figure 3C) and detected transitive siRNAs in sense and antisense orientation (Figure 3D). Thus, biogenesis of transitive siRNAs in *P. patens* differs from biogenesis of secondary siRNAs in *C. elegans*, as these occur in antisense polarity only because of unprimed de novo synthesis by RdRP (Pak and Fire, 2007; Sijen et al., 2007).

DNA Methylation of Genes Encoding miRNA Targets in Δ*PpDCL1b*

A. thaliana ago1 and *dcl1* mutants are defective in miRNA-directed cleavage or miRNA biogenesis, respectively, and thus overaccumulate miRNA target transcripts (Ronemus et al., 2006). Conversely, in Δ*PpDCL1b*, all miRNA targets analyzed had reduced levels (Figure 4A and Figure S5A), although transcripts were not cleaved. These unexpected findings hint at an epigenetic control of genes encoding miRNA targets. Since methylation of cytosine residues is associated with transcriptional silencing in eukaryotes (Bender, 2004), we performed methylation-specific PCR from five loci, four encoding miRNA targets and one encoding *PpGNT1* (Figures 4B–4E, Figure S5B, and Figure S6A–S6E). Promoters of the five genes were unmethylated in the WT, whereas in Δ*PpDCL1b* the four promoters of miRNA targets were methylated, but not the promoter of *PpGNT1* (Figure 4C). This was confirmed by sequencing the PCR products from the *PpARF* promoter, demonstrating no methylation in the WT and methylation of CpG residues in Δ*PpDCL1b* (Figure S6A). Taken together, our experiments

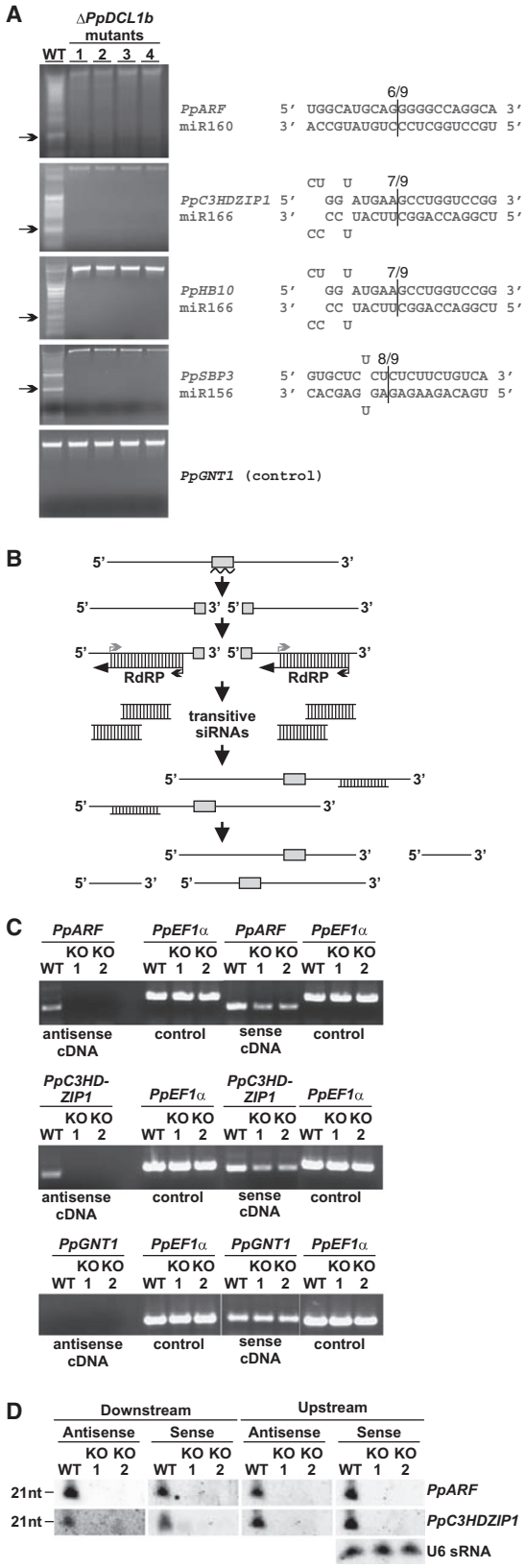

Figure 3. RNA Cleavage Products, Antisense Transcripts, and Transitive siRNAs

(A) 5′ RACE products of miRNA targets and a control transcript (*PpGNT1*) from the WT and Δ*PpDCL1b*. Arrows mark products of the size expected for cleavage products that were eluted, cloned, and sequenced. Numbers above miRNA:target alignments indicate sequenced RACE products with the corresponding 5′ end.

(B) Scheme for the generation of transitive siRNAs. DsRNA is synthesized from cleaved miRNA targets by RdRP, processed into transitive siRNAs that mediate cleavage of the target RNA upstream and downstream of the miRNA recognition motif. Black line, mRNA; gray box, miRNA binding site; curved line, miRNA. Arrows indicate primers for RT-PCR, with gray indicating primers for cDNA synthesis from antisense strand and black for sense strand.

(C) RT-PCR products derived from antisense or sense-specific cDNAs from the WT and two Δ*PpDCL1b* mutants (KO1 and KO2).

(D) Detection of sense and antisense transitive siRNAs derived from *PpARF* and *PpC3HDZIP1* RNAs using hybridization probes targeting regions upstream and downstream of the miRNA binding sites. U6snRNA served as a control.

See Figure S4 for complete images of blots including size markers.

show that targeted disruption of the *PpDCL1b* gene led to loss of miRNA-directed mRNA cleavage accompanied by specific epigenetic changes in genes encoding miRNA targets.

While it is well known that siRNA pathways govern DNA methylation in *A. thaliana*, e.g., at repeat-associated loci (Cokus et al., 2008; Herr et al., 2005; Lister et al., 2008), only one study suggests a function of miRNAs in gene silencing: normally methylated DNA sequences downstream of the miRNA complementary motif became hypomethylated in plants with dominant alleles of *PHB* and *PHV*, encoding targets of miR165/166, while the promoters remained unmethylated (Bao et al., 2004). The dominant alleles alter the miRNA targeting motif, so that the mRNAs are no longer miRNA targets. Like *AtPHB* and *AtPHV*, the moss genes *PpC3HDZIP1* and *PpHB10* harbor an intron in the miRNA binding site (Figure S5B), whereas the miRNA targeting motif of *PpARF* is not disrupted. Similar to the promoters, *PpC3HDZIP1* and *PpARF* sequences flanking the miRNA targeting motif as well as the disrupting intron in *PpC3HDZIP1* were CpG methylated in Δ*PpDCL1b* but not in the WT (Figures 4D and 4E, and Figure S6B–S6E).

To study whether this hypermethylation in Δ*PpDCL1b* leads to transcriptional silencing, we performed nuclear run-ons. When compared to the WT, transcription rates of genes encoding miRNA targets were reduced in Δ*PpDCL1b*, whereas transcription rates of the unmethylated *PpGNT1* control gene were similar in the WT and mutants (Figure 4F and Figure S6F). Thus, we conclude that hypermethylation of genes encoding miRNA targets in Δ*PpDCL1b* downregulates their expression, hence accounting for the reduced levels of their mature RNAs.

A possible scenario for these findings is that PpDCL1b is pivotal for a cleavage competent RISC and that in Δ*PpDCL1b* miRNAs are not loaded to RISC but to an RNA-induced transcriptional silencing (RITS) complex that induces methylation and subsequent downregulation of the corresponding genes. As the sequences encoding the future miRNA binding site are disrupted by introns in *PpC3HDZIP1* and *PpHB10* it is unlikely that their methylation in Δ*PpDCL1b* is initiated by miRNA:DNA hybrids. Instead, the miRNA-loaded RITS complex may interact with target mRNAs forming stable miRNA:mRNA duplexes.

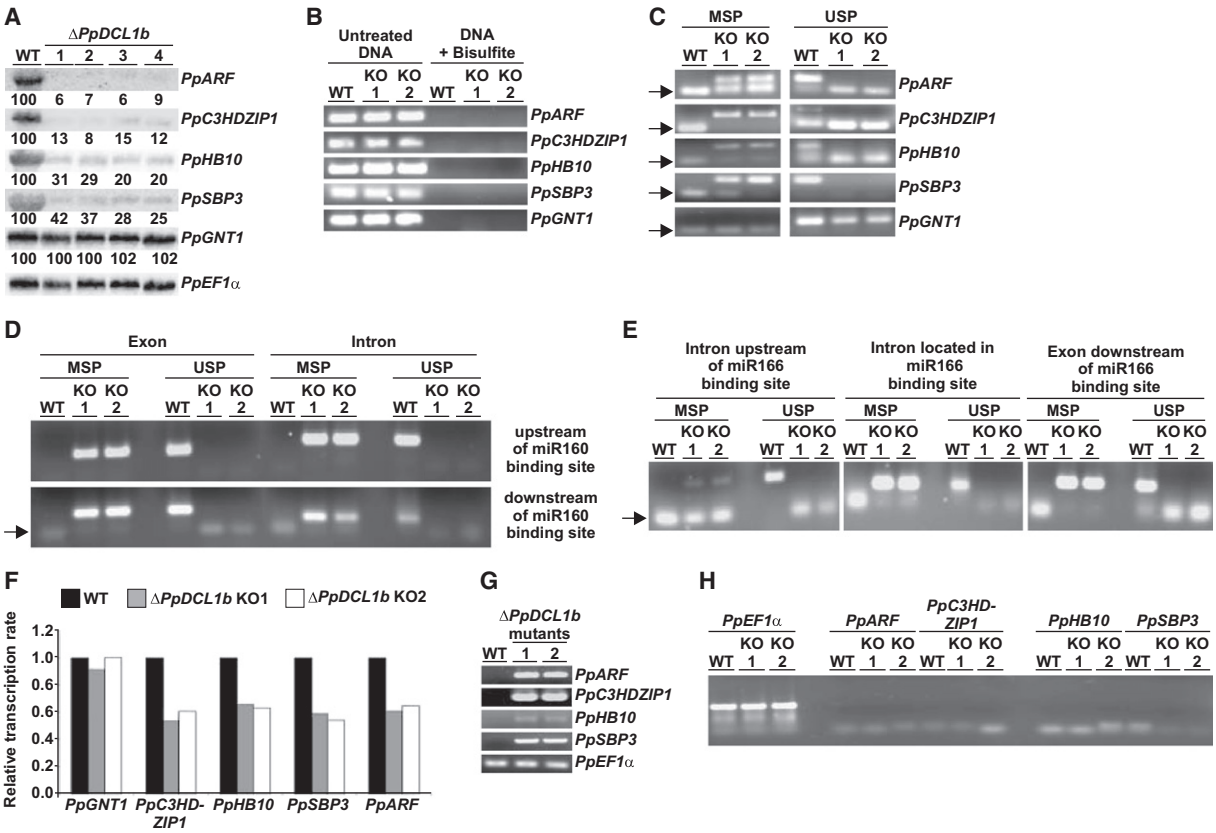

Figure 4. Expression of miRNA Target Genes, DNA Methylation, and miRNA:mRNA Duplexes

(A) RNA blot analysis of genes encoding miRNA targets (*PpARF*, *PpC3HDZIP1*, *PpHB10*, *PpSBP3*) and control genes (*PpGNT1* and *PpEF1α*) in the WT and Δ*PpDCL1b* mutants (1–4). Hybridization signals were normalized to *PpEF1α* and transcript levels relative to the WT are indicated. See Figure S5A for an independent expression analysis by qRT-PCR.

(B) Specificity analysis of bisulfite PCR using primers specific for unmodified sequences. PCR was performed with untreated and bisulfite-treated genomic DNA of the WT and two Δ*PpDCL1b* mutants (KO1 and KO2).

(C–E) PCR reactions with bisulfite-treated genomic DNA using methylation-specific (MSP) and unmethylation-specific (USP) primers.

(C) Bisulfite PCR for promoters of genes encoding miRNA targets and the *PpGNT1* control.

(D) Bisulfite PCR analysis of *PpARF* sequences surrounding the miR160 targeting motif. See Figure S5B for gene structures and Figure S6A–S6E for nucleotide sequences of PCR products obtained from bisulfite PCR of the *PpARF* gene.

(E) Bisulfite PCR analysis of *PpC3HDZIP1* sequences upstream of, the intron disrupting, and downstream of the miR166 targeting motif. Arrows in (C)–(E) mark primer bands.

(F) Relative transcription rates of genes encoding miRNA targets and of *PpGNT1* in the WT and in Δ*PpDCL1b* determined by nuclear run-ons. Hybridization signals were normalized to *PpEF1α* and transcription rates in the WT were set to 1. See Figure S6F for images of hybridized membranes.

(G) PCR products of miRNA targets using cDNA synthesized from the WT and two Δ*PpDCL1b* mutants (1 and 2) without exogenous primers. For the *PpGNT1* control PCR products were detected from neither the WT nor Δ*PpDCL1b* (data not shown). A *PpEF1α* primer for cDNA synthesis was added as internal control to all reactions.

(H) The same experiment performed with RNA samples that had been heated for 5 min to 95°C prior to cDNA synthesis. The control *PpEF1α* primer was added after cooling of the RNA samples.

Subsequently, these duplexes could guide the RITS complex to the corresponding genomic regions, initiate and spread DNA methylation.

If stable miRNA:mRNA duplexes exist, they should prime cDNA synthesis without exogenous primers. In support of this scenario, we obtained RT-PCR products from unprimed cDNA synthesis for all miRNA targets examined but not for a control transcript in Δ*PpDCL1b*. No such products were obtained with RNA from the WT (Figure 4G). In addition, from Δ*PpDCL1b* no PCR products were obtained with primers located downstream of the miRNA targeting site. As a further control, we heated the RNA samples prior to cDNA synthesis. This should lead to denaturation of miRNA:mRNA complexes and hence eliminate priming. Indeed, this setup prevented amplification of PCR products from Δ*PpDCL1b* (Figure 4H). These findings point at the presence of base-paired miRNA:mRNA duplexes in Δ*PpDCL1b* but not in the WT.

To further scrutinize our hypotheses of transitivity and miRNA-dependent DNA methylation, we analyzed the ta-siRNA pathway. After miR390-mediated cleavage of *TAS* precursors the RNA cleavage products are converted into dsRNA and further processed into ta-siRNAs (Axtell et al., 2006; Talmor-Neiman

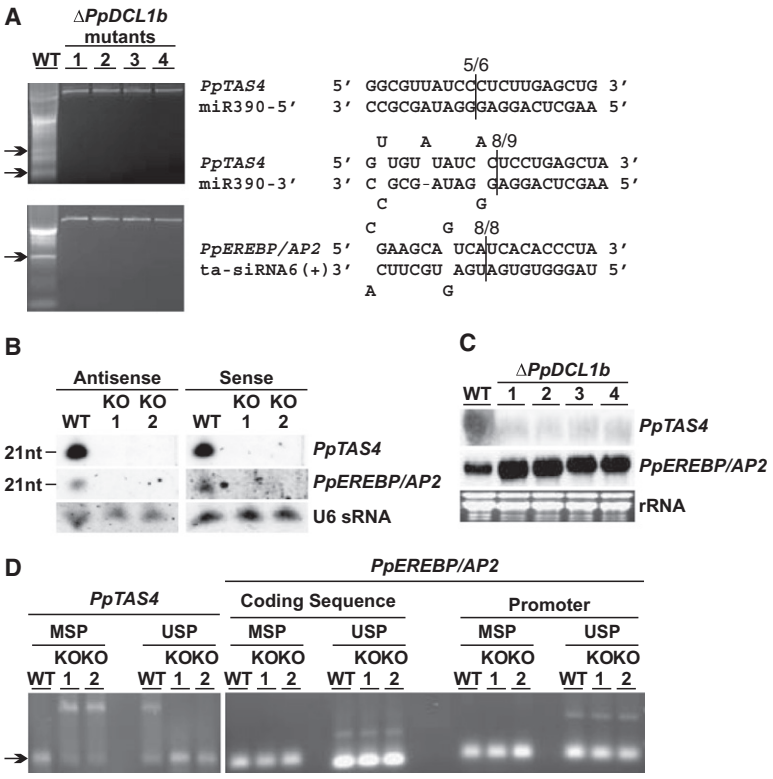

Figure 5. The ta-siRNA Pathway

(A) 5′ RACE-PCRs from the WT and Δ*PpDCL1b* mutants (1–4) for miR390 target *PpTAS4* and ta-siRNA target *PpEREBP/AP2*. Arrows mark products of the size expected for cleavage products that were eluted from the gel, cloned, and sequenced. The number of sequenced RACE-PCR products with the corresponding 5′ end is indicated above the alignment.

(B) ta-siRNAs derived from *PpTAS4* and transitive siRNAs derived from *PpEREBP/AP2*. U6snRNA served as a control. See Figure S7 for complete images of blots including size markers.

(C) RNA blots for *PpTAS4* and *PpEREBP/AP2* transcripts. EtBr staining as loading control below.

(D) Bisulfite PCR with methylation-specific (MSP) and unmethylation-specific (USP) primers for *PpTAS4* and *PpEREBP/AP2*. Arrow marks primer dimers.

et al., 2006). In *P. patens*, the mRNA encoding an *EREBP/AP2* transcription factor is targeted by one of the ta-siRNAs derived from the *TAS4* precursor (Talmor-Neiman et al., 2006). *TAS4* RNA cleavage products were detected by 5′ RACE-PCR in the WT but not in Δ*PpDCL1b* (Figure 5A), although miR390 was present in equal amounts in both (Figure 2C). Furthermore, ta-siRNAs of both sense and antisense orientation were present in the WT but undetectable in Δ*PpDCL1b* (Figure 5B and Figure S7), confirming the requirement of PpDCL1b for initiation of the ta-siRNA pathway.

In agreement with our findings for other miRNA targets, *TAS4* transcript levels were reduced (Figure 5C) and the *TAS4* gene was methylated in Δ*PpDCL1b* only (Figure 5D). If, similar to miRNAs, ta-siRNA-mediated cleavage of target RNAs initiates the generation of transitive siRNAs, the lack of ta-siRNAs in Δ*PpDCL1b* should abolish both cleavage of *EREBP/AP2* mRNA and generation of transitive siRNAs. Consistent with this, *EREBP/AP2* mRNA was cleaved in the WT but not in Δ*PpDCL1b* (Figure 5A), and only the WT produced *EREBP/AP2* mRNA-derived siRNAs in sense and antisense orientation (Figure 5B and Figure S7). These observations indicate that siRNA-dependent amplification of target RNA degradation initially triggered by ta-siRNA- or miRNA-guided cleavage is a common phenomenon in *P. patens*. In addition, in contrast to direct miRNA targets, *EREBP/AP2* mRNA levels should be elevated in Δ*PpDCL1b*, as stable ta-siRNA:mRNA duplexes that could initiate silencing of the corresponding gene should be absent. Indeed, *EREBP/AP2* mRNA levels were increased in Δ*PpDCL1b* (Figure 5C) and the corresponding gene was methylated in neither the WT nor Δ*PpDCL1b* (Figure 5D).

Dependence of DNA Methylation on miRNA Levels

We propose that miRNA:target-RNA duplexes lead to methylation and subsequent downregulation of the corresponding genes in Δ*PpDCL1b*. To gain more insight into this mechanism, we generated transgenic lines that express different levels of an artificial miRNA (amiRNA) targeting the control gene *PpGNT1*.

An amiRNA against *PpGNT1* was engineered into the *A. thaliana* miR319a precursor (Khraiwesh et al., 2008) and transfected into the WT and Δ*PpDCL1b* (Figure 6A). RNA blots confirmed precise maturation of amiR-GNT1 in the transformed lines, independent of expression level (Figure 6B and Figure S8D). The expected *PpGNT1* mRNA cleavage products were present in the WT and absent in Δ*PpDCL1b* (Figure 6C). As a consequence, *PpGNT1* transcript levels were reduced in amiR-GNT1 WT plants and even lower in the Δ*PpDCL1b* background, despite abolished amiRNA-directed cleavage of *PpGNT1* RNA in the latter (Figure 6D). Consistent with our model of miRNA-dependent epigenetic silencing, the *PpGNT1* promoter was methylated in Δ*PpDCL1b* (Figure 6E and Figure S8A). Beyond that, we observed methylation of this promoter in a WT line with high amiR-GNT1expression levels (line #2) but not in a line with low amiR-GNT1 levels (line #1) (Figure 6E and Figure S8A). Thus, methylation and subsequent silencing of miRNA target loci is not limited to Δ*PpDCL1b* but also occurs in the *P. patens* WT and is miRNA-dosage dependent.

Therefore, we hypothesized that the ratio of a miRNA to its target RNA is crucial for induction of DNA methylation at the target locus. If miRNA concentrations exceed a threshold, the miRNA may either interact directly with its target and the duplex might then be recruited to a DNA methylation silencing complex or the excess miRNA might be loaded into an effector complex such as RITS, triggering duplex formation that directs DNA methylation. We obtained supporting evidence for the expected amiR-GNT1:*PpGNT1*-mRNA duplexes by cDNA synthesis without exogenous primers and subsequent PCR from Δ*PpDCL1b* and from a WT line with high levels of amiRNAs while this was impossible from a WT line accumulating moderate amounts of amiR-GNT1 (Figure 6F).

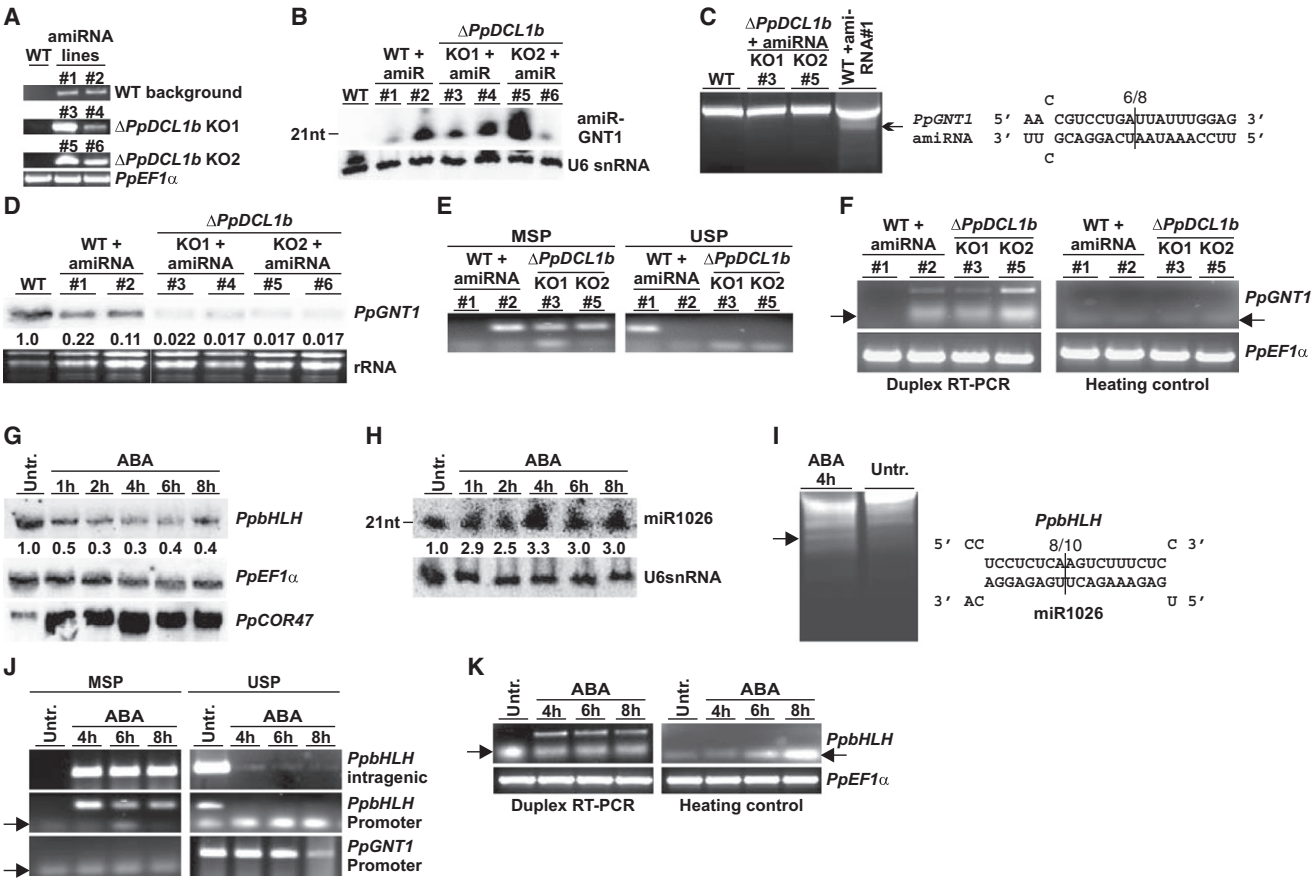

Figure 6. Lines Expressing amiR-GNT1 and Analysis of miR1026 Target *PpbHLH*

(A) PCR-based identification of transgenic lines harboring a *PpGNT1*-amiRNA expression construct in the WT (lines #1 and #2), Δ*PpDCL1b* mutant 1 (lines #3 and #4), and Δ*PpDCL1b* mutant 2 (lines #5 and #6) backgrounds. *PpEF1α* served as a control.

(B) Detection of amiR-GNT1 by RNA blot loaded with 50 μg total RNA. U6snRNA served as a control. See Figure S8D for complete images of blots including size markers.

(C) Cleavage mapping of *PpGNT1* in amiR-GNT1 lines by 5′ RACE-PCR. The number of sequenced RACE-PCR products with the corresponding 5′ end is indicated above the alignment.

(D) RNA blot of WT and amiR-GNT1 lines probed for *PpGNT1*. Hybridization signals were normalized to rRNA. Levels relative to the WT are indicated.

(E) Bisulfite PCR on genomic DNA from amiR-GNT1 lines using methylation-specific (MSP) and unmethylation-specific (USP) primers derived from the *PpGNT1* promoter. See Figure S8A for nucleotide sequences of PCR products obtained from bisulfite PCR.

(F) RT-PCR to detect amiR-GNT1:*PpGNT1*-mRNA duplexes using cDNA synthesized without exogenous primers. PCR was carried out with a primer pair upstream of the amiR-GNT1 target motif. Amplification controls as in Figures 4G and 4H. Arrows mark primer dimers.

(G) RNA blots with 20 μg total RNA from untreated (Untr.) and ABA-treated WT using probes for *PpbHLH*, the loading control *PpEF1α* and *PpCOR47*, a known ABA-induced gene. *PpbHLH* levels were normalized to *PpEF1α*. Relative *PpbHLH* RNA levels compared to the WT are given.

(H) RNA blot with 50 μg total RNA from untreated (Untr.) and ABA-treated WT. MiR1026 levels were normalized to U6snRNA. Numbers indicate miR1026 levels relative to the WT. See Figure S8D for complete images of blots including size markers.

(I) 5′ RACE-PCR for *PpbHLH* using RNA from untreated (Untr.) and WT treated for 4 hr with ABA. Arrows mark products of the size expected for cleavage products that were eluted from the gel, cloned, and sequenced. Numbers above miRNA:target alignments indicate sequenced RACE-PCR products with the corresponding 5′ end.

(J) Bisulfite PCR reactions on DNA from untreated (Untr.) and ABA-treated WT with methylation-specific (MSP) and unmethylation-specific (USP) primers targeting *PpbHLH* genomic sequences. *PpGNT1* promoter served as control. Arrows mark primer dimers. See Figures S8B and S8C for nucleotide sequences of PCR products obtained from bisulfite PCR.

(K) RT-PCR to detect miR1026:*PpbHLH*-mRNA duplexes using cDNA synthesized without exogenous primers. PCR was carried out with a primer pair upstream of the miR1026 binding site. Amplification controls as in Figure 4G and 4H. Arrows mark primer dimers.

Hormone-Dependent DNA Methylation

So far, we have found evidence for miRNA-directed epigenetic silencing in a knockout mutant and in a transgenic WT that ectopically expresses high levels of an amiRNA. If the proposed mechanism of gene regulation is of general relevance, at least in moss, it should be detectable in the nontransgenic WT under physiological conditions as well.

The plant hormone abscisic acid (ABA) represses mRNA levels of a gene (*PpbHLH*) encoding a basic helix-loop-helix transcription factor (Richardt et al., 2009). The *PpbHLH* mRNA was

predicted as target of miR1026 (Axtell et al., 2007). ABA is a potent regulator of abiotic stress signaling pathways in plants including moss (Frank et al., 2005b). Northern blots confirmed downregulation of *PpbHLH* in response to ABA (Figure 6G). This effect correlated with an ABA-induced increase of miR1026 levels (Figure 6H and Figure S8D). MiR1026-mediated cleavage of *PpbHLH* transcripts was confirmed by 5′ RACE (Figure 6I), revealing a regulatory circuit between ABA, *PpbHLH*, and miR1026. Further, upon ABA treatment, the *PpbHLH* gene was methylated at CpG sites (Figure 6J, and Figures S8B and S8C), mirroring the methylation patterns we found in Δ*PpDCL1b* and in the WT ectopically expressing high levels of amiRNA. The promoter of the control gene *PpGNT1* was unmethylated in the nontransgenic WT regardless of ABA treatment (Figure 6J). However, under these physiological conditions, methylation of the *PpbHLH* gene was not quantitative, as unmethylation-specific primers allowed some, albeit inefficient, PCR amplifications from ABA-treated samples. These findings appear to support our model, as we propose that DNA methylation is initiated only if miRNA levels exceed a threshold. In line with this, we obtained evidence for stable miR1026:*PpbHLH*-mRNA duplexes by unprimed RT-PCR. Consistent with the DNA methylation status, such duplexes were only found in ABA-treated samples (Figure 6K).

DISCUSSION

We have shown that in *P. patens* epigenetic silencing of genes encoding miRNA target RNAs contributes to the control of gene expression. Although we initially discovered this phenomenon in Δ*PpDCL1b*, subsequent analyses of the miR1026/*PpbHLH* regulon confirmed that this type of miRNA-dependent transcriptional control operates also in the WT under physiological conditions.

Our studies suggest that PpDCL1a is the functional ortholog of AtDCL1 required for miRNA and ta-siRNA biogenesis. Although PpDCL1b shares a similar level of sequence identity, it has a different function, as its deletion does not affect miRNA biogenesis but abolishes miRNA-directed target cleavage. It is unlikely that PpDCL1b directly cleaves RNAs as AGO proteins in RISC are the catalytic enzymes in sRNA-dependent target cleavage (MacRae et al., 2008). Biochemical analysis of AGO1 complexes from *A. thaliana dcl1-7*, *dcl2-1* and *dcl3-1* mutants provided evidence for distinct functional properties. An AGO1 complex extracted from *dcl1-7* mutants was not able to cleave RNA targets because of the lack of ~21 nt RNA accumulation in this mutant. In contrast, cleavage of RNA targets was not affected in AGO1 complexes from *dcl2-1* and *dcl3-1* mutants (Qi et al., 2005). Furthermore, purification of AtAGO1 revealed an ~160 kDa complex, most likely only consisting of AGO1 and associated sRNA (Baumberger and Baulcombe, 2005). Thus, there is so far no evidence for a role of plant DCL proteins in sRNA-mediated target cleavage. In contrast, studies in animals have shown that Dicer proteins are part of the RNA loading complex (RLC) that loads sRNAs into RISC. Human RLC comprises the proteins Ago2, Dicer, and TRBP, and the purified components assemble spontaneously in vitro without any cofactors. The reconstituted RLC is functional and once Ago2 is loaded with a miRNA it dissociates from the rest of the complex (MacRae et al., 2008). Similarly, Dcr-2 from *D. melanogaster*, which produces siRNA, acts in RISC assembly together with R2D2 by loading one of the two siRNA strands into RISC (Liu et al., 2003; Tomari et al., 2004). The *C. elegans* homolog of this protein, RDE-4, likewise interacts with Dicer (Tabara et al., 2002). Given this particular function of animal Dicers, *P. patens* DCL1b may equivalently act in loading miRNAs into RISC. Whatever the precise function of this protein is, our results revealed its pivotal role for miRNA-directed target cleavage.

As we found no transitive siRNAs derived from miRNA and ta-siRNA targets in Δ*PpDCL1b*, it is tempting to speculate that PpDCL1b is involved in the generation of these siRNAs. *A. thaliana* DCL2 is essential for transitive silencing of transgenes (Mlotshwa et al., 2008; Moissiard et al., 2007). As no AtDCL2 homolog is encoded by the *P. patens* genome, PpDCL1b may function in siRNA production. Although we cannot exclude the possibility that PpDCL1b generates transitive siRNAs from double-stranded miRNA and ta-siRNA targets, we favor the scenario that miRNA-mediated cleavage of transcripts is essential for the onset of transitivity in *P. patens* and that the lack of transitive siRNAs in Δ*PpDCL1b* is caused by a lack of miRNA target cleavage.

In *A. thaliana dcl1* and *ago1* mutants, which are affected in miRNA biogenesis or miRNA-directed target cleavage, respectively, levels of miRNA targets are elevated (Ronemus et al., 2006). Likewise, levels of miRNA targets are increased in Δ*PpDCL1a* because of the lack of miRNAs. In contrast, levels of miRNA targets are drastically reduced in Δ*PpDCL1b*, in spite of abolished target cleavage. We found methylation of the corresponding genes in these mutants, suggesting together with evidence from nuclear run-ons an epigenetic control at the transcriptional level. Small RNAs initiate transcriptional silencing of homologous sequences by methylation of cytosine residues at CpG, CpNpG, and CpHpH motifs or by histone modifications (Bender, 2004; Cao and Jacobsen, 2002). In all genes analyzed in Δ*PpDCL1b*, we solely detected methylation at CpG, although we cannot exclude that methylation also occurs in different sequence contexts in other regions. Moreover, we detected methylation of the genes encoding miRNA targets in introns, exons, and promoters, pointing to methylation that is able to spread over long distances.

Although spreading of siRNA-directed DNA methylation into adjacent nonrepeated sequences is not common in *A. thaliana*, siRNA-mediated spreading of DNA methylation was found in the *SUPPRESSOR OF drm1 drm2 cmt3* (SDC) locus, where methylation spreads beyond siRNA generating repeat regions present in the promoter (Henderson and Jacobsen, 2008). In *A. thaliana*, methylation can also spread in the *PHV* and *PHB* genes that are targets of miR165/166 (Bao et al., 2004). In both genes, the miR165/166 complementary motif is disrupted by an intron and the coding sequences were heavily methylated downstream of the miRNA complementary site in differentiated but not in undifferentiated cells of WT plants. Furthermore, methylation is reduced in *phv-1d* and *phb-1d* mutants, which have an altered miRNA recognition motif or a mutation in the intron splice donor sequence, suggesting that miR165/166 needs to bind

to nascent *PHV* and *PHB* transcripts to trigger gene silencing (Bao et al., 2004).

Similarly, the *P. patens* genes *PpC3HDZIP1* and *PpHB10* are targeted by miR166 and its binding sites are only reconstituted after splicing of the primary transcripts. Both loci are hypermethylated in Δ*PpDCL1b* but not in the WT, suggesting that initiation of methylation upon defective target cleavage is not mediated by miR166 but involves interaction of miR166 with its target RNAs. We obtained evidence for the presence of stable duplexes of a miRNA and its target RNA in Δ*PpDCL1b* and propose that these duplexes guide a DNA modification complex.

In *A. thaliana* RNA-directed DNA methylation (RdRM) by siRNAs requires RDR2, DCL3, and RNA PolIVa, which are all involved in siRNA biogenesis (Herr et al., 2005; Kanno et al., 2005; Onodera et al., 2005; Pontier et al., 2005; Xie et al., 2004), whereas AGO4, DRM2, DRD1, and RNA PolIVb are necessary for DNA methylation (Cao and Jacobsen, 2002; Kanno et al., 2005; Zilberman et al., 2004). *P. patens* encodes six AGO homologs (Axtell et al., 2007). Three of them cluster with AGO1 from *A. thaliana* and are under control of miR904, reminiscent of the autoregulatory control of *AtAGO1* by miR168. Thus, it is likely that they are components of a *P. patens* miRNA-RISC. The other three moss AGO paralogs cluster with *Arabidopsis* AGO6, AGO4, AGO9, and AGO8 (supported by a bootstrap value of 99). Thus, it is unclear which of these *P. patens* proteins is functionally equivalent to AtAGO4. Furthermore, we cannot rule out functional redundancies between them.

In fission yeast, RNA-directed heterochromatic gene silencing at centromeres relies on two complexes, the RITS complex with Ago1, Chp1, and TAS3, and the Argonaute siRNA chaperone complex (ARC) with Ago1, Arb1, and Arb2. However, these complexes are required to direct histone methylation, but do not trigger DNA methylation. Nevertheless, it was suggested that their action involves the recognition of nascent transcripts by RITS-bound siRNAs to promote recruitment of chromatin-modifying enzymes that implement silencing (Bühler et al., 2006; Motamedi et al., 2004). So far, chromatin immunoprecipitation with subsequent unprimed RT-PCR was not successful in our hands, most probably because heat-induced reversal of crosslinking also denatures miRNA:RNA duplexes. Thus, it remains open whether the miRNA:target-RNA duplexes observed here form from nascent or from mature transcripts.

We detected specific silencing of genes encoding miRNA targets not only in a targeted knockout mutant but also in the *P. patens* WT, where the expression of amiR-GNT1 caused methylation of *PpGNT1*. Methylation of this gene was dependent on high amiR-GNT1 abundance. Likewise, amiR-GNT1:*PpGNT1*-mRNA duplexes were characteristic for lines with high amiRNA levels, supporting the model that miRNA:target-RNA duplexes are required for gene-specific DNA methylation. Finally, we found that the *PpbHLH* gene encoding a miR1026 target was methylated in response to ABA. As with amiR-GNT1 and its target, DNA methylation was miR1026 dosage-dependent and appeared to correlate with the formation of miR1026:*PpbHLH*-mRNA duplexes. As ABA is a mediator of abiotic stress signaling, we suggest that miR1026-regulated silencing of *PpbHLH* is part of stress adaptation in the *P. patens* WT under physiological conditions.

In plants, epigenetic changes in response to stress include DNA methylation, histone modifications, and chromatin remodeling (Boyko and Kovalchuk, 2008; Dyachenko et al., 2006; Henderson and Dean, 2004). In addition to that, our analysis of the miR1026:*PpbHLH* regulon suggests that miRNAs also act in the epigenetic control of stress-responsive genes.

Taken together, we propose that epigenetic gene silencing can be triggered by duplexes of a miRNA and its target RNA, being either an mRNA or a primary *TAS* transcript. This transcriptional control of genes encoding miRNA target RNAs discovered in *P. patens* presents a new mechanism to affect the homeostasis of miRNA-regulated RNAs (Figure 7). Recently, two studies found an involvement of miRNAs in transcriptional gene silencing in mammals (Gonzalez et al., 2008; Kim et al., 2008) but the proposed mechanisms differ from the model presented here. The precursor of human miR-320 is encoded in antisense orientation proximal to the transcription start site of the *POL3RD* gene, suggesting a *cis*-regulatory function of miR-320. Evidence for this scenario was obtained from transfection of HEK293 cells with miR-320 which caused transcriptional silencing of *POL3RD* (Kim et al., 2008). Epigenetic changes such as DNA methylation or histone modifications were not analyzed (Kim et al., 2008). Gonzalez et al. (2008) reported on the role of mammalian miRNAs in repressing promoter activity, which requires promoter-overlapping transcription and the presence of miRNA seed-matches in the transcribed strand of the promoter. In addition to quite different underlying mechanisms of miRNA action, we note that these studies relied solely on ectopic expression of miRNAs in cell culture.

Our model entails that the specific equilibrium of a cleavage-competent RISC and a DNA-modifying RITS loaded with the same miRNA determines the relative contribution of both pathways to miRNA-mediated downregulation of gene expression in *P. patens*. In addition, siRNA-mediated transitivity as a major factor in amplifying the original miRNA- and ta-siRNA-directed cleavage signal appears to be more prevalent in this moss than in *A. thaliana*. It seems not unlikely that similar modifications and specializations of RNAi pathways will be found in other eukaryotes as well.

EXPERIMENTAL PROCEDURES

Plant Material

Culture of *P. patens*, transformation, and molecular analyses were performed according to Frank et al. (2005a). For hormone treatment 10 μM (±)-*cis-trans* ABA was added to *P. patens* liquid cultures. Δ*PpDCL1a* mutants were propagated on full medium (Egener et al., 2002).

Generation of Δ*PpDCL1a* and Δ*PpDCL1b* Mutants

An *nptII* cassette was cloned into single restriction sites present in *PpDCL1a* and *PpDCL1b*, respectively. The gene disruption constructs were transfected into *P. patens* protoplasts and G418-resistant lines were analyzed by PCR to confirm precise integration into the targeted genes. Loss of *PpDCL1a* and *PpDCL1b* transcript, respectively, was confirmed by RT-PCR. The generation of Δ*PpDCL1a* and Δ*PpDCL1b* mutants is described in detail in the Extended Experimental Procedures and Figures S1 and S2.

P. patens Expressing amiR-GNT1

The generation of an amiRNA targeting *PpGNT1* was described previously (Khraiwesh et al., 2008). The amiRNA expression construct was transfected

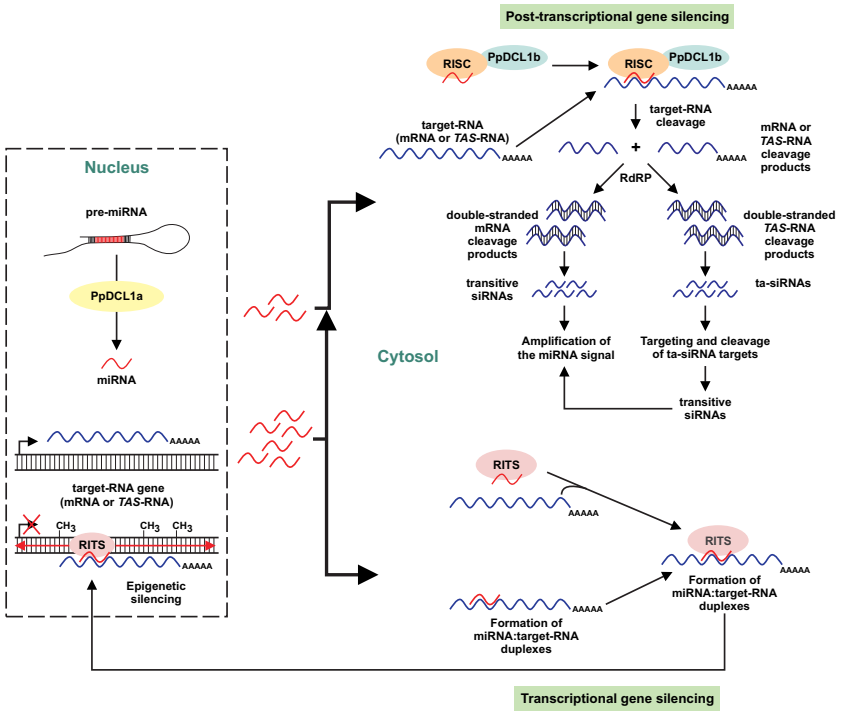

Figure 7. Model for Posttranscriptional and Transcriptional Silencing of Genes Encoding miRNA Targets

Whereas PpDCL1a acts in miRNA biogenesis, PpDCL1b is pivotal for a cleavage-competent RISC. At low miRNA:target-RNA ratios, gene expression is regulated posttranscriptionally via RISC. After loading of miRNAs into RISC, miRNA:target-RNA duplexes form on the basis of sequence complementarities, resulting in target RNA cleavage. Amplification of the miRNA signal by transitive siRNAs occurs. Targeted deletion of the *PpDCL1b* gene abolishes this pathway in the mutant and leads to gene silencing via RITS. In the WT, hormone treatment enhances miRNA levels and thus increases miRNA:target-RNA ratios. In addition to loading miRNA into RISC, miRNAs form duplexes with their target RNAs. Highly abundant miRNAs are either loaded into a RITS complex and subsequently interact with their target to form a duplex, or these duplexes are formed at first and then loaded into RITS. The miRNA:RNA duplexes bound by RITS initiate DNA methylation at complementary genomic loci. The RITS complex is able to spread CpG methylation over the entire locus.

into the *P. patens* WT and Δ*PpDCL1b*. The generation of amiR-GNT1-expressing lines is described in detail in the Extended Experimental Procedures.

RT-PCR of Small RNAs

RT-PCR analyses of miRNAs and ta-siRNAs was carried out as described (Varkonyi-Gasic et al., 2007). Primers for cDNA synthesis and subsequent PCR reactions are reported in Table S1.

DNA Methylation Analysis

DNA sequences were analyzed with the MethPrimer program (Li and Dahiya, 2002) to deduce methylation-specific (MSP) and unmethylation-specific (USP) primers for PCR of bisulfite-treated DNA. Two micrograms of genomic DNA were used for sodium bisulfite treatment with the EpiTect Bisulfite Kit (QIAGEN). DNA methylation analysis and primer sequences are reported in Table S1.

Nuclear Run-on Assay

Isolation of nuclei from 4 g protonema of the *P. patens* WT and two Δ*PpDCL1b* mutants and subsequent run-on transcription assays using 3×10^6 nuclei each were carried out according to Folta and Kaufman (2006). Radiolabeled RNA was hybridized to blots spotted with 3 μg of denatured gene-specific cDNA fragments of *PpEF1α*, *PpGNT1*, *PpC3HDZIP1*, *PpHB10*, *PpSBP3*, and *PpARF* and a negative control cDNA fragment of the bacterial zeocin gene (*Sh ble*), respectively. Blot hybridization was carried out at 65°C in 0.05 M sodium phosphate (pH 7.2), 1 mM EDTA, 6× SSC, 1× Denhardt's, and 5% SDS. Blots were washed at 65°C twice with 2× SSC and 0.2% SDS and once with 1× SSC and 0.1% SDS. Hybridization signals were quantified with the Quantity One Software and normalized to *PpEF1α*. Oligonucleotides for amplification of cDNA fragments are reported in Table S1.

Detection of miRNA:mRNA Duplexes

CDNA was synthesized from 4 μg total RNA with Superscript III (Invitrogen) without adding primers, except a primer specific for the *PpEF1α* transcript to monitor cDNA synthesis efficiency. Gene-specific primers located upstream of miRNA binding sites that were used for RT-PCRs are reported in Table S1.

SUPPLEMENTAL INFORMATION

Supplemental Information includes Extended Experimental Procedures, eight figures, and one table and can be found with this article online at doi:10.1016/j.cell.2009.12.023.

ACKNOWLEDGMENTS

This work was supported by Landesstiftung Baden-Württemberg (P-LS-RNS/40 to D.W., W.F., and R.R.), the German Federal Ministry of Education and Research (FRISYS 0313921 to W.F. and R.R.), the Excellence Initiative of the German Federal and State Governments (EXC 294 to R.R.), the European Community FP6 IP SIROCCO (LSHG-CT-2006-037900 to D.W.), and the German Academic Exchange Service (DAAD to M.A.A.). We thank G. Gierga and R. Haas for technical assistance, K.M. Folta for advice on nuclear run-ons, and T. Laux, W.R. Hess, R. Baumeister, and P. Beyer for comments on the manuscript.

Received: October 15, 2008
Revised: July 30, 2009
Accepted: November 28, 2009
Published: January 7, 2010

REFERENCES

Arazi, T., Talmor-Neiman, M., Stav, R., Riese, M., Huijser, P., and Baulcombe, D.C. (2005). Cloning and characterization of micro-RNAs from moss. Plant J. *43*, 837–848.

Axtell, M.J., Jan, C., Rajagopalan, R., and Bartel, D.P. (2006). A two-hit trigger for siRNA biogenesis in plants. Cell *127*, 565–577.

Axtell, M.J., Snyder, J.A., and Bartel, D.P. (2007). Common functions for diverse small RNAs of land plants. Plant Cell *19*, 1750–1769.

Bao, N., Lye, K.W., and Barton, M.K. (2004). MicroRNA binding sites in *Arabidopsis* class III HD-ZIP mRNAs are required for methylation of the template chromosome. Dev. Cell *7*, 653–662.

Baulcombe, D. (2004). RNA silencing in plants. Nature *431*, 356–363.

Baumberger, N., and Baulcombe, D.C. (2005). Arabidopsis ARGONAUTE1 is an RNA Slicer that selectively recruits microRNAs and short interfering RNAs. Proc. Natl. Acad. Sci. USA *102*, 11928–11933.

Bender, J. (2004). Chromatin-based silencing mechanisms. Curr. Opin. Plant Biol. *7*, 521–526.

Boyko, A., and Kovalchuk, I. (2008). Epigenetic control of plant stress response. Environ. Mol. Mutagen *49*, 61–72.

Bühler, M., Verdel, A., and Moazed, D. (2006). Tethering RITS to a nascent transcript initiates RNAi- and heterochromatin-dependent gene silencing. Cell *125*, 873–886.

Cao, X., and Jacobsen, S.E. (2002). Locus-specific control of asymmetric and CpNpG methylation by the DRM and CMT3 methyltransferase genes. Proc. Natl. Acad. Sci. USA *99* (*Suppl 4*), 16491–16498.

Carthew, R.W., and Sontheimer, E.J. (2009). Origins and Mechanisms of miRNAs and siRNAs. Cell *136*, 642–655.

Cokus, S.J., Feng, S., Zhang, X., Chen, Z., Merriman, B., Haudenschild, C.D., Pradhan, S., Nelson, S.F., Pellegrini, M., and Jacobsen, S.E. (2008). Shotgun bisulphite sequencing of the *Arabidopsis* genome reveals DNA methylation patterning. Nature *452*, 215–219.

Doi, N., Zenno, S., Ueda, R., Ohki-Hamazaki, H., Ui-Tei, K., and Saigo, K. (2003). Short-interfering-RNA-mediated gene silencing in mammalian cells requires Dicer and eIF2C translation initiation factors. Curr. Biol. *13*, 41–46.

Duchaine, T.F., Wohlschlegel, J.A., Kennedy, S., Bei, Y., Conte, D., Jr., Pang, K., Brownell, D.R., Harding, S., Mitani, S., Ruvkun, G., et al. (2006). Functional proteomics reveals the biochemical niche of *C. elegans* DCR-1 in multiple small-RNA-mediated pathways. Cell *124*, 343–354.

Dunoyer, P., Himber, C., and Voinnet, O. (2005). DICER-LIKE 4 is required for RNA interference and produces the 21-nucleotide small interfering RNA component of the plant cell-to-cell silencing signal. Nat. Genet *37*, 1356–1360.

Dyachenko, O.V., Zakharchenko, N.S., Shevchuk, T.V., Bohnert, H.J., Cushman, J.C., and Buryanov, Y.I. (2006). Effect of hypermethylation of CCWGG sequences in DNA of *Mesembryanthemum crystallinum* plants on their adaptation to salt stress. Biochemistry (Mosc.) *71*, 461–465.

Egener, T., Granado, J., Guitton, M.C., Hohe, A., Holtorf, H., Lucht, J.M., Rensing, S.A., Schlink, K., Schulte, J., Schween, G., et al. (2002). High frequency of phenotypic deviations in *Physcomitrella patens* plants transformed with a gene-disruption library. BMC Plant Biol. *2*, 6.

Fattash, I., Voss, B., Reski, R., Hess, W.R., and Frank, W. (2007). Evidence for the rapid expansion of microRNA-mediated regulation in early land plant evolution. BMC Plant Biol. *7*, 13.

Floyd, S.K., and Bowman, J.L. (2004). Gene regulation: ancient microRNA target sequences in plants. Nature *428*, 485–486.

Folta, K.M., and Kaufman, L.S. (2006). Isolation of *Arabidopsis* nuclei and measurement of gene transcription rates using nuclear run-on assays. Nat. Protoc. *1*, 3094–3100.

Frank, W., Decker, E.L., and Reski, R. (2005a). Molecular tools to study *Physcomitrella patens*. Plant Biol (Stuttg) *7*, 220–227.

Frank, W., Ratnadewi, D., and Reski, R. (2005b). *Physcomitrella patens* is highly tolerant against drought, salt and osmotic stress. Planta *220*, 384–394.

Gasciolli, V., Mallory, A.C., Bartel, D.P., and Vaucheret, H. (2005). Partially redundant functions of *Arabidopsis* DICER-like enzymes and a role for DCL4 in producing trans-acting siRNAs. Curr. Biol. *15*, 1494–1500.

Golden, T.A., Schauer, S.E., Lang, J.D., Pien, S., Mushegian, A.R., Grossniklaus, U., Meinke, D.W., and Ray, A. (2002). SHORT INTEGUMENTS1/SUSPENSOR1/CARPEL FACTORY, a Dicer homolog, is a maternal effect gene required for embryo development in *Arabidopsis*. Plant Physiol. *130*, 808–822.

Gonzalez, S., Pisano, D.G., and Serrano, M. (2008). Mechanistic principles of chromatin remodeling guided by siRNAs and miRNAs. Cell Cycle *7*, 2601–2608.

Henderson, I.R., and Dean, C. (2004). Control of *Arabidopsis* flowering: the chill before the bloom. Development *131*, 3829–3838.

Henderson, I.R., and Jacobsen, S.E. (2008). Tandem repeats upstream of the *Arabidopsis* endogene SDC recruit non-CG DNA methylation and initiate siRNA spreading. Genes Dev. *22*, 1597–1606.

Henderson, I.R., Zhang, X., Lu, C., Johnson, L., Meyers, B.C., Green, P.J., and Jacobsen, S.E. (2006). Dissecting *Arabidopsis thaliana* DICER function in small RNA processing, gene silencing and DNA methylation patterning. Nat. Genet. *38*, 721–725.

Herr, A.J., Jensen, M.B., Dalmay, T., and Baulcombe, D.C. (2005). RNA polymerase IV directs silencing of endogenous DNA. Science *308*, 118–120.

Howell, M.D., Fahlgren, N., Chapman, E.J., Cumbie, J.S., Sullivan, C.M., Givan, S.A., Kasschau, K.D., and Carrington, J.C. (2007). Genome-wide analysis of the RNA-DEPENDENT RNA POLYMERASE6/DICER-LIKE4 pathway in *Arabidopsis* reveals dependency on miRNA- and tasiRNA-directed targeting. Plant Cell *19*, 926–942.

Kanno, T., Huettel, B., Mette, M.F., Aufsatz, W., Jaligot, E., Daxinger, L., Kreil, D.P., Matzke, M., and Matzke, A.J. (2005). Atypical RNA polymerase subunits required for RNA-directed DNA methylation. Nat. Genet. *37*, 761–765.

Khraiwesh, B., Ossowski, S., Weigel, D., Reski, R., and Frank, W. (2008). Specific gene silencing by artificial MicroRNAs in *Physcomitrella patens*: an alternative to targeted gene knockouts. Plant Physiol. *148*, 684–693.

Kim, D.H., Saetrom, P., Snøve, O., Jr., and Rossi, J.J. (2008). MicroRNA-directed transcriptional gene silencing in mammalian cells. Proc. Natl. Acad. Sci. USA *105*, 16230–16235.

Koprivova, A., Altmann, F., Gorr, G., Kopriva, S., Reski, R., and Decker, E.L. (2003). N-glycosylation in the moss *Physcomitrella patens* is organized similarly to that in higher plants. Plant Biol. *5*, 582–591.

Li, L.C., and Dahiya, R. (2002). MethPrimer: designing primers for methylation PCRs. Bioinformatics *18*, 1427–1431.

Lister, R., O'Malley, R.C., Tonti-Filippini, J., Gregory, B.D., Berry, C.C., Millar, A.H., and Ecker, J.R. (2008). Highly integrated single-base resolution maps of the epigenome in *Arabidopsis*. Cell *133*, 523–536.

Liu, Q., Rand, T.A., Kalidas, S., Du, F., Kim, H.E., Smith, D.P., and Wang, X. (2003). R2D2, a bridge between the initiation and effector steps of the *Drosophila* RNAi pathway. Science *301*, 1921–1925.

Luo, Q.J., Samanta, M.P., Köksal, F., Janda, J., Galbraith, D.W., Richardson, C.R., Ou-Yang, F., and Rock, C.D. (2009). Evidence for antisense transcription associated with microRNA target mRNAs in *Arabidopsis*. PLoS Genet. *5*, e1000457.

MacRae, I.J., Ma, E., Zhou, M., Robinson, C.V., and Doudna, J.A. (2008). In vitro reconstitution of the human RISC-loading complex. Proc. Natl. Acad. Sci. USA *105*, 512–517.

Matzke, M., Kanno, T., Huettel, B., Daxinger, L., and Matzke, A.J. (2007). Targets of RNA-directed DNA methylation. Curr. Opin. Plant Biol. *10*, 512–519.

Mlotshwa, S., Pruss, G.J., Peragine, A., Endres, M.W., Li, J., Chen, X., Poethig, R.S., Bowman, L.H., and Vance, V. (2008). DICER-LIKE2 plays a primary role in transitive silencing of transgenes in Arabidopsis. PLoS ONE *3*, e1755.

Moissiard, G., Parizotto, E.A., Himber, C., and Voinnet, O. (2007). Transitivity in *Arabidopsis* can be primed, requires the redundant action of the antiviral Dicer-like 4 and Dicer-like 2, and is compromised by viral-encoded suppressor proteins. RNA *13*, 1268–1278.

Motamedi, M.R., Verdel, A., Colmenares, S.U., Gerber, S.A., Gygi, S.P., and Moazed, D. (2004). Two RNAi complexes, RITS and RDRC, physically interact and localize to noncoding centromeric RNAs. Cell *119*, 789–802.

Onodera, Y., Haag, J.R., Ream, T., Nunes, P.C., Pontes, O., and Pikaard, C.S. (2005). Plant nuclear RNA polymerase IV mediates siRNA and DNA methylation-dependent heterochromatin formation. Cell *120*, 613–622.

Pak, J., and Fire, A. (2007). Distinct populations of primary and secondary effectors during RNAi in C. elegans. Science *315*, 241–244.

Park, W., Li, J., Song, R., Messing, J., and Chen, X. (2002). CARPEL FACTORY, a Dicer homolog, and HEN1, a novel protein, act in microRNA metabolism in *Arabidopsis thaliana*. Curr. Biol. *12*, 1484–1495.

Pham, J.W., Pellino, J.L., Lee, Y.S., Carthew, R.W., and Sontheimer, E.J. (2004). A Dicer-2-dependent 80s complex cleaves targeted mRNAs during RNAi in *Drosophila*. Cell *117*, 83–94.

Pontier, D., Yahubyan, G., Vega, D., Bulski, A., Saez-Vasquez, J., Hakimi, M.A., Lerbs-Mache, S., Colot, V., and Lagrange, T. (2005). Reinforcement of silencing at transposons and highly repeated sequences requires the concerted action of two distinct RNA polymerases IV in *Arabidopsis*. Genes Dev. *19*, 2030–2040.

Qi, Y., Denli, A.M., and Hannon, G.J. (2005). Biochemical specialization within *Arabidopsis* RNA silencing pathways. Mol. Cell *19*, 421–428.

Richardt, S., Timmerhaus, G., Lang, D., Qudeimat, E., Corrêa, L.G., Reski, R., Rensing, S.A., and Frank, W. (2010). Microarray analysis of the moss *Physcomitrella patens* reveals evolutionarily conserved transcriptional regulation of salt stress and abscisic acid signalling. Plant Mol. Biol *72*, 27–45.

Ronemus, M., Vaughn, M.W., and Martienssen, R.A. (2006). MicroRNA-targeted and small interfering RNA-mediated mRNA degradation is regulated by argonaute, dicer, and RNA-dependent RNA polymerase in *Arabidopsis*. Plant Cell *18*, 1559–1574.

Sijen, T., Steiner, F.A., Thijssen, K.L., and Plasterk, R.H. (2007). Secondary siRNAs result from unprimed RNA synthesis and form a distinct class. Science *315*, 244–247.

Strepp, R., Scholz, S., Kruse, S., Speth, V., and Reski, R. (1998). Plant nuclear gene knockout reveals a role in plastid division for the homolog of the bacterial cell division protein FtsZ, an ancestral tubulin. Proc. Natl. Acad. Sci. USA *95*, 4368–4373.

Tabara, H., Yigit, E., Siomi, H., and Mello, C.C. (2002). The dsRNA binding protein RDE-4 interacts with RDE-1, DCR-1, and a DExH-box helicase to direct RNAi in *C. elegans*. Cell *109*, 861–871.

Talmor-Neiman, M., Stav, R., Klipcan, L., Buxdorf, K., Baulcombe, D.C., and Arazi, T. (2006). Identification of trans-acting siRNAs in moss and an RNA-dependent RNA polymerase required for their biogenesis. Plant J. *48*, 511–521.

Tomari, Y., and Zamore, P.D. (2005). Perspective: machines for RNAi. Genes Dev. *19*, 517–529.

Tomari, Y., Matranga, C., Haley, B., Martinez, N., and Zamore, P.D. (2004). A protein sensor for siRNA asymmetry. Science *306*, 1377–1380.

Vaistij, F.E., Jones, L., and Baulcombe, D.C. (2002). Spreading of RNA targeting and DNA methylation in RNA silencing requires transcription of the target gene and a putative RNA-dependent RNA polymerase. Plant Cell *14*, 857–867.

Varkonyi-Gasic, E., Wu, R., Wood, M., Walton, E.F., and Hellens, R.P. (2007). Protocol: a highly sensitive RT-PCR method for detection and quantification of microRNAs. Plant Methods *3*, 12.

Voinnet, O. (2009). Origin, biogenesis, and activity of plant microRNAs. Cell *136*, 669–687.

Xie, Z., Johansen, L.K., Gustafson, A.M., Kasschau, K.D., Lellis, A.D., Zilberman, D., Jacobsen, S.E., and Carrington, J.C. (2004). Genetic and functional diversification of small RNA pathways in plants. PLoS Biol. *2*, E104.

Xie, Z., Allen, E., Wilken, A., and Carrington, J.C. (2005). DICER-LIKE 4 functions in trans-acting small interfering RNA biogenesis and vegetative phase change in *Arabidopsis thaliana*. Proc. Natl. Acad. Sci. USA *102*, 12984–12989.

Zilberman, D., Cao, X., Johansen, L.K., Xie, Z., Carrington, J.C., and Jacobsen, S.E. (2004). Role of *Arabidopsis* ARGONAUTE4 in RNA-directed DNA methylation triggered by inverted repeats. Curr. Biol. *14*, 1214–1220.